DESIGN OF A SYSTEM TO STUDY HUMAN INTERNAL DISC STRAINS IN TORSION AND COMPRESSION MEASURED NONINVASIVELY USING MAGNETIC RESONANCE IMAGING

NSF Summer Undergraduate Fellowship in Sensor Technologies
Valerie, Walters (ESM) – Virginia Polytechnic Institute and State University
Advisor: Dawn M. Elliot, PhD

ABSTRACT

Many people suffer from lower back pain, which can be caused by disc degeneration. We are studying the properties of non-degenerated and degenerated human lumbar intervertebral discs. The overall objective of this study is to quantify strains in the disc when it is under torsional and compressive loading, simultaneously. This will be done by using magnetic resonance images of discs before and after loading and advanced normalization tools, which is an image normalization technology. For this summer, the objective is to design a device that will load the specimen as previously described and be compatible with the magnetic resonance imaging machine. The protocol will consist of incrementally torquing the specimen while in constant compression. The torque and the compressive force will be monitored via a load cell throughout the test. We expect displacement results to agree with previous studies that have been done in standard mechanical testing equipment. We also hypothesize that the outer annulus fibrous will be the stiffest part of the disc, and that the posterior region will be stiffer than the anterior region. The strain results that we expect to obtain do not have a previous test to compare to; this is the first study that will quantify internal disc strains while the disc is in torsion. We expect the results to provide useful information about the properties of the human intervertebral disc.

Table of Contents

1. INTRODUCTION

Disc degeneration in the human lumbar spine has been studied over the last decades. It continues to receive attention from the biomechanics and biomedical fields because it is believed to be a main source of lower back pain [1] [2]. Approximately 65 million Americans experience lower back pain per year [3], and Americans alone spend around fifty billion dollars each year on back pain [4].

Compression and torsion are both looked at when studying disc degeneration because these are two types of forces that act on the intervertebral disc. The spinal column is usually under compression of one's body weight; the function of the disc is to behave like a shock absorber and to distribute the stress and strain [5]. The disc also functions like a pivot point [5], which allows us to turn; this movement creates torsion on the disc. Past experiments have shown that discs simultaneously in torsion and compression can injure the spine's facet joints [1]. In another study it was shown, in vivo, that degeneration of the intervertebral disc (IVD) led to a decrease in torsional motion [6]. These previous studies, along with others [7] [8] [9], help lead to the conclusion that torsional movement, also known as axial rotation, is greatly affected by disc degeneration [9].

Previous studies done on the human lumbar spine in torsion include measuring the rotation when a known torque is applied for normal discs [10], measuring the stiffness / rotation of the discs when a known torque is applied for both normal and degenerated discs [7] [8] [9], and measuring maximum torque and rotation for both normal and degenerated discs [6]. While these previous provide useful information, they have certain limitations. These limitations include the use of physical markers and not applying a compressive load. Using physical markers can disrupt the disc's structural integrity, alter the deformation of the disc, and move separately from the tissue [11]. In vivo, the spine is in compression; therefore, a non-weight bearing study, in vitro, does not represent the spine's natural loading. Isolation of the disc was done in some studies and can be seen as a limitation depending on the ultimate goal of the research. Isolating the disc consists of removing the joints, tendons, and ligaments; while this is done in many studies, for example [6] [10]. However, isolation can be seen as a limitation because the facet joints are one of the key elements in the stability of the intervertebral disc [9], and the facet joints resist most of the torque loading, which causes them to experience yielding before the disc does [12]. On the other hand, if the properties of interest are related to the disc alone, isolating the disc is not a limitation.

The objective of this entire study is to quantify strain due to torsion and compression, simultaneously, noninvasively by using a combination of MRI and advanced normalization tools (ANTS), an image normalization technology. Strain due to compression was first quantified by O'Connell *et al* in 2007 [11], but strain due to torsion has yet to be quantified. This study will apply a constant compressive load along with incremental torsional loads. Both normal and degenerated isolated discs will be looked at during this study. The goal of this study is to better understand the disc's properties; therefore, the disc will be isolated. The tests will be conducted on individual cadaveric spinal motion segments, bone-disc-bone.

We hypothesize that the outer annulus fibrosus will be stiffer than the inner annulus fibrosus, which will be stiffer than the nucleus pulposus. We also expect that the anterior portion and the posterior portion of the disc to have the same stiffness. Our final hypothesis is that non-degenerated discs will be stiffer than degenerated discs, which has been shown in previous tests [7].

The project is in the early design stages. The objective of this summer's project is to design a device that will be able to load the specimen in torsion and compression, simultaneously. This device will also be able to be placed into a magnetic resonance imaging (MRI) machine. The goal for the completion of the device design is early August of this year. Preliminary testing can be done in the lab, outside the MRI machine, during the design stage. Preliminary tests will give information on the stress-relaxation times at various angle displacements. Tests for materials strength and durability will also be done when needed for the design. This will be an ongoing study for the next few months in order to collect sufficient data and analyze the results.

Section 2 of this paper gives background on disc degeneration, disc anatomy for both normal and degenerated discs, magnetic resonance imaging, and texture correlation. Section 3 of this paper discusses the design of the device. Section 4 then discusses the materials and methods that will be used for the upcoming study. Section 5 will discuss the preliminary testing results, if applicable. Section 6 will then discuss the limitations to this study, and then Section 7 will give the conclusions of this paper.

2. BACKGROUND

2.1 Disc Degeneration

Disc degeneration does not have just one definition; in fact, it includes the following features: alterations in the structure, cell-mediated changes, pain, and advanced signs of aging [1] [2]. Disc degeneration becomes more common with age, but is not to be confused with signs of aging. A key difference between the two is that degeneration increases metabolite transfer to the discs structure, whereas age decreases it [2]. Approximately 85% of people will show signs of disc degeneration by the time they reach the age of 50 [3]. Disc degeneration can be caused by factors such as mechanical loading [1] [2] and processes that inhibit the healing process [2]. However, the leading cause of disc degeneration is genetics. Between 50-70% of those affected by disc degeneration genetically inherited the trait [2].

2.2 Disc Anatomy

2.2.1 Normal Disc

A human intervertebral disc is the soft tissue between the spine's vertebrae. The IVDs function as shock absorbers and pivot points. The disc is also responsible for distributing the stress and strain evenly throughout the disc [5]. The discs are thickest in the lumbar

region, which supports the majority of the strain from the rest of the spine [5]. A disc is made up of endplates, the nucleus pulposus, and the annulus fibrosus [11].

The endplates of the spinal column separate the discs. The annulus fibrosus is composed mostly of lamellae, which is made of collagen fibers [2]. The nucleus pulposus is located in the center of the disc and is surrounded by the annulus fibrosus. The nucleus pulposus is a white substance composed of loose, wavy, gelatinous fibers [5]. See Figure 1 for a cross-sectional view of a human intervertebral disc [13]. The nucleus pulposus is generally under compression, which creates a tensile hoop stress on the annulus fibrosus. The pressurization of nucleus pulposus is responsible for maintaining disc height, transmitting the compressive load, and preventing large deformations [14].

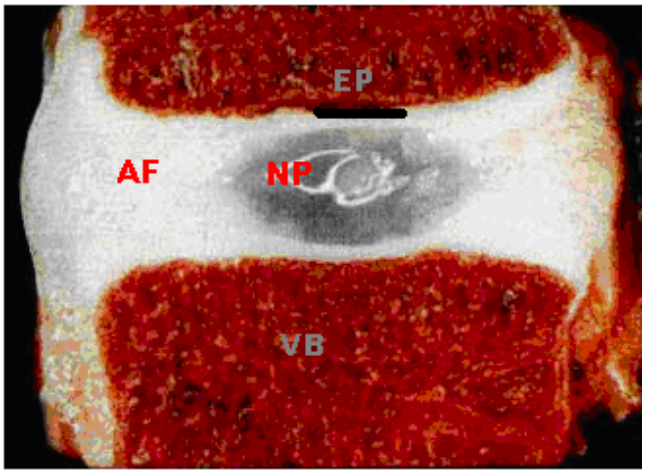

Figure 1: Cross-sectional view of a human intervertebral disc [13], where NP represents the nucleus pulposus, AF represents the annulus fibrosus, EP represents an end plate, and VB represents the vertebral body.

2.2.2 Degenerated Disc

The anatomy of an intervertebral disc changes during degeneration. Early stages of degeneration are marked with a loss of proteoglycan content [14] [15] [16], which reduces the nucleus pulposus' ability to attract and bind water [15] [16]. The loss of hydration causes a decrease in the hydrostatic pressure of the nucleus pulposus [14] [15] [16]. The loss of hydration in the nucleus pulposus makes it a semi gelatinous structure instead of a pure gelatinous structure. This results in a less obvious distinction between the annulus fibrosus and the nucleus pulposus [5] and the disc behaves more like an elastic solid than a viscoelastic fluid [17]. Other physiological changes that occur in a degenerated disc include a decrease in disc height, radial tears and/or rim lesions [15]. See Figure 2 for a cross-sectional view of a degenerated human intervertebral disc [18].

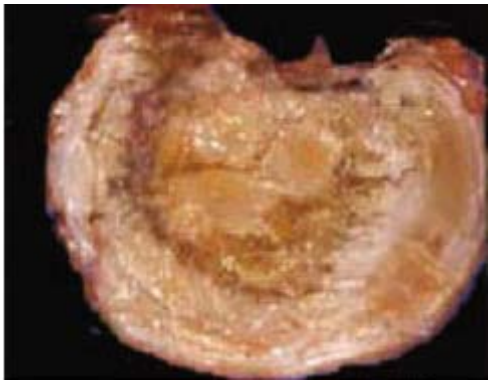

Figure 2: Cross-section view of a degenerative human intervertebral disc [18].

To determine the severity of disc degeneration, MR images of the discs are graded using a T_2 or $T_{1\rho}$ grading system. T_2 is a quantitative method and is more widely known, used, and accepted system. T_2 is the older system, whereas $T_{1\rho}$ is a newer system that is more sensitive to early stages of degeneration because it measures the loss of proteoglycan content [14] [15] [16]. The T_2 system is an integer-based system with grades from 1 to 5, where 1 is associated with a non-degenerated disc and 5 is associated with a severely degenerated disc [16]. Since the T_2 system is integer-based, it makes it prone to observer bias [15]. The $T_{1\rho}$ system uses a spin-lock technique and does not require any invasive biomarkers [14] [16]. $T_{1\rho}$ also uses a continuous scale, which reduces observer bias and makes its dynamic range larger than the T_2 range [15]. See Figure 3 below for a comparison between the T_2 and $T_{1\rho}$ images [15].

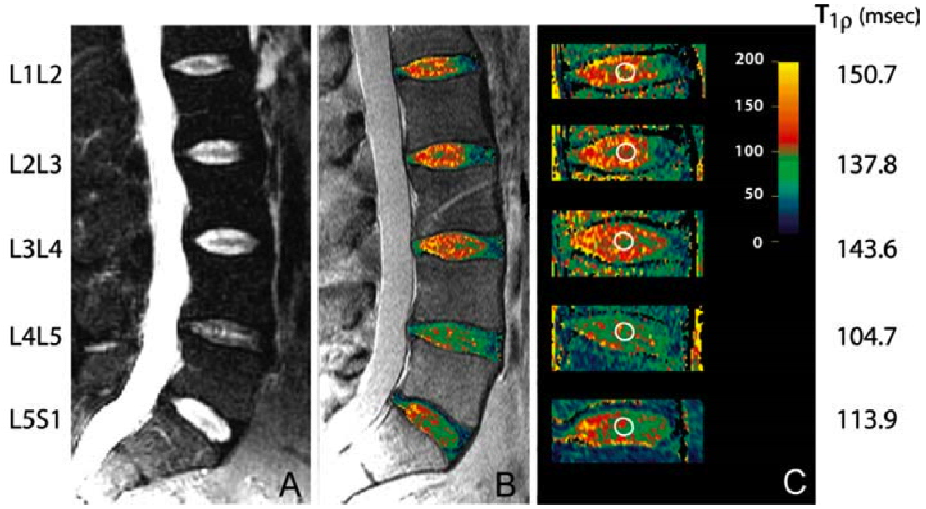

Figure 3: A) T_2-weighted images B) $T_{1\rho}$ images and C) enlarged maps from the $T_{1\rho}$ images [15].

2.2.3 Diurnal Effects

Throughout the day disc height decreases. The total disc height decrease in the entire spine is on average 19 mm, which corresponds to approximately 1.5 mm height change in each lumbar disc [17]. The height change is associated with loss of fluid content, approximately 5-10% [19], due to compressive stresses throughout the day. At night, when there is minimal loading on the spine, the discs rehydrate and increase in height. Ludescher *et al* determined that there were no morphological changes in the disc when comparing images from the morning and the evening in the same individuals [19]. However, it has been shown that the spine is stiffer in the mornings, reducing the lumbar flexion range by approximately 5°, and it has been shown that the disc resists more of the stress in the morning [17]. Degenerated discs lose the ability to fully rehydrate during rest [19] [20]. Many in vivo studies have been done to look at the diurnal effects, such as [19] [20] [21] [22] [23].

2.3 Magnetic Resonance Imaging

The advantage of using magnetic resonance imaging (MRI) for internal strain studies is that it does not require the use of physical markers. Chiu *et al* stated that since the intervertebral disc has a high water content it is a good area to use MRI; however, the location of the intervertebral disc makes it difficult to use MRI in vivo [24]. Nevertheless, MRI has been accepted as a valid and accurate method to use when imaging specimens. This method has been used in many previous studies, for example [7] [8] [9] [11] [24] [25]; however, to date MRI has not been used for internal strain measurements except by the McKay Orthopedic Research Laboratory.

3. MATERIALS AND METHODS

The summer's objective was to design a device that will apply compression and torsion, simultaneously, to a spinal motion segment. The criteria of the device include: MRI compatible, measure the torque and compression throughout the test, and control the amount of torque and compression independently. Currently, there is no system that is capable of accomplishing the project's needs; therefore, a new design was needed.

This section includes details on the entire project, but mostly focuses on the design of the device.

3.1 Sample Preparation

Human cadaveric spine sections will be obtained from an IRB approved tissue source. Before dissection, T_2-weighted and $T_{1\pm\rho}$ images will be obtained for the whole spine. From these images, the degenerative grade of the discs will be determined based on the Pfirrmann scale [29]. From the spine, the lumbar motion segments, bone-disc-bone, will be used. The disc will be isolated, meaning the facet joints and other ligaments will be removed. Kirschner wires will be placed through the vertebral bodies, and then the motion segments will be potted in polymethyl methacrylate (PMMA) bone cement. The

specimens will be stored at -20°C until needed. In order to hydrate the specimen, the specimen will be placed in a phosphate buffered saline (PBS) bath in a refrigerator for 15 hours then at room temperature in a PBS bath 3 hours prior to testing.

3.2 Custom Built Device

3.2.1 Preliminary Design

At the beginning of this project, the objective was to study the effects of just torsion on strain of the intervertebral disc. In order to measure the torque being applied to the specimen, it was decided that a load cell would be used. The load cell would have to be rotating with the specimen. An actuator would also be needed in order to apply a rotational movement. Ideally, the device would be small and lightweight since it would have to be moved from the lab to an MRI machine. Another obstacle that was present was to keep the metal approximately 8 inches away from the specimen to eliminate any imaging interference. This distance, 8 inches, was chosen because it was slightly greater than the minimum distance between a hydraulic cylinder and the specimen for a compression device that is currently used in the MRI.

With that in mind, it was decided to load the specimen in a device that would keep one side completely stationary. Four polyvinyl chloride (PVC) plastic rods with a diameter of 0.25 inches would be used to transfer the torque from the rotary actuator to the specimen. The interface between the rotary actuator and the specimen would be a thin rectangular block. Holes would be drilled through the PMMA that was connected to the specimen in order for the rods to slide through. Another rod would be used to transfer the torque from the specimen back to the load cell, which would be mounted on the rotating rectangle. Figure 4 below gives an idea of what the device would look like; however, Figure 4 does not show the load cell or the load cell connection.

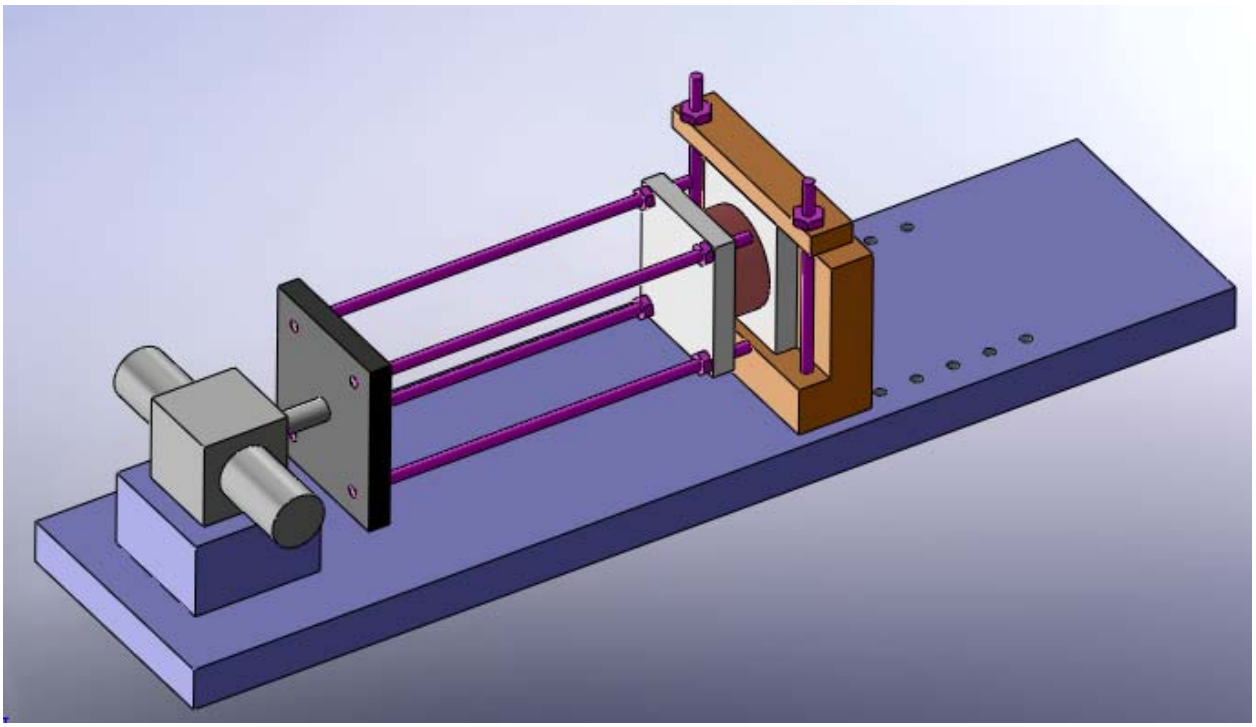

Figure 4: A picture created in Solidworks 2008 shows the preliminary design. The blue shows the base; purple shows the rods; the orange shows the supports; the gray shows the PMMA; the red shows the motion segment; the black shows the rotating rectangle; the silver shows the rotary actuator.

3.2.2 Design Issues

While working on the preliminary design, some issues arose. The 0.25-inch diameter PVC rods were not stiff enough to resist the amount of torque; it was also noted that the torque would have to be applied in the opposite directions of the threads in order for the rods to transfer the rotation. The small diameter was chosen because, originally, it was thought that the tooling to transfer the torque needed to be as lightweight as possible in order for the rotary actuator to perform as expected. However, after talking with Doug Hamilton, a representative from Bimba, the manufacturer of the rotary actuator selected, it was determined that the weight of the tooling was not a large issue, but bending moment could affect the performance.

As this project progressed, it was decided that torsion and compression would be studied simultaneously, instead of just torsion. Therefore, a way to add compression to the device would have to be designed. It was also decided to incrementally increase the torque. This will increase the length of the test, which makes hydration of the specimen an issue. Another issue that arose was the distance the metal had to be from the specimen in order to get quality images. After meeting with Niels Oesingmann, a contractor from Siemens, which is the manufacturer of the both the 3T and the 7T MRI machine that might be used, it is thought that the load cell will have the greatest effect on the image quality, but the required minimum distances vary for each application. It was also noted that the orientation of each device could change the required minimum distance. A protocol was

developed to determine the minimum distances for each device. The protocol is described below in Section 3.3.

3.2.3 Current Design

A non-magnetic custom device is being designed that will apply torsion and axial compression, simultaneously, to a motion segment while in the MRI machine. The device will consist of a custom-built load cell to measure the torque and compression on the motion segment (LXT-920, Cooper Instruments), a custom-built rotary actuator (Bimba), and a stainless steel hydraulic cylinder (URR-17-1/2, Clippard Minimatic) that will apply compression. One pressurized nitrogen tank will control the rotary actuator, and another pressurized nitrogen tank will control the hydraulic cylinder. An accurate release of nitrogen will be required from these tanks; the valves to control the release of nitrogen have not been determined at this point. All other parts of the device will be made of PVC and Delrin plastics.

The load cell will be on one side of the specimen and the rotary actuator and the hydraulic cylinder will be placed on the other side. The wires from the load cell will be twisted and wrapped in order to help isolate them in order to reduce their interference. Since the weight of the tooling is no longer an issue, thicker rods, with a diameter of 1 inch, made of Delrin plastic will be used to transfer the torque and rotation from the rotary actuator to the specimen and then from the specimen to the load cell; only one rod will be used on each side. In order to reduce bending moment effects, each rod will have at least one support with a ball bearing. The number of supports depends on the length of the rods, which is currently unknown but will be decided from the results from the protocol described in Section 3.3. The ball bearings will be made of plastic and glass (ARG16-1B-G, KMS Bearings, Inc.). The specimen will be gripped using t-slots made from Delrin plastic. The motion segment will slide into one piece of the grips and then be secured by Delrin screws. That piece will then slide into the other part of the t-slot, which will have a stopper to keep it from being off-centered. The t-slot will connect to the rods via Delrin screws. In order to keep the specimen hydrated, it will be submerged in a PBS bath; this should not affect the image quality.

Compression is being added to the device by the use of a hydraulic cylinder. Two design options were made to add compression to the device. For both options, the compressive hydraulic cylinder will be located behind the rotary actuator. One option, which is shown in Figure 5, has the hydraulic cylinder applying compression to the back of the rotary actuator support. The support would be allowed to slide and the compression would be transferred through the same rods that the torque and rotation would be transferred. The disadvantage to this option is the small surface area for the compression to be applied to the specimen. The second option, shown in Figure 6, has the hydraulic cylinder applying compression to a bar, which is connected to two 0.5-inch square rods made of Delrin plastic. These square rods extend on the outside of the rotary actuator to a PVC rectangular block, which will be adjacent to the grips of the specimen. The PVC block will have a circular cutout either larger than the diameter of the Delrin rod or a bearing will be placed in the cutout in order to transfer the rotation without adding friction. This

design mimics the compression device that has previously been used. This design option increases the surface area for compression, but the issue is the Delrin rod would have to extend.

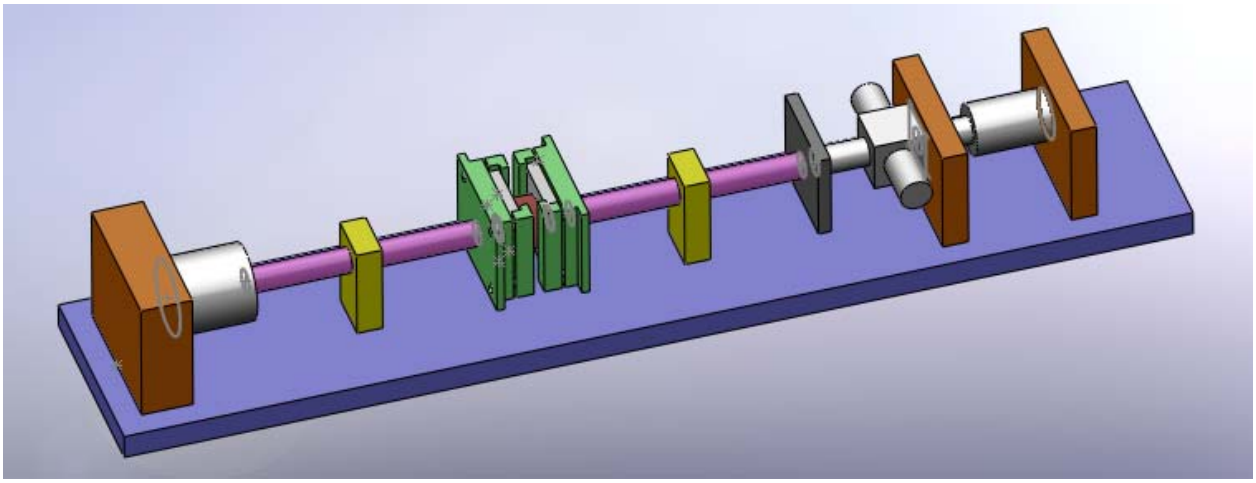

Figure 5: A picture created in Solidworks 2008 shows one of the design options. The blue shows the base; purple shows the rods; the orange shows the supports; the green shows the grips; the gray shows the PMMA; the red shows the motion segment; the black shows the rotating rectangle; the silver shows the devices (load cell, rotary actuator, hydrualic cylinder); the yellow shows the bearing supports.

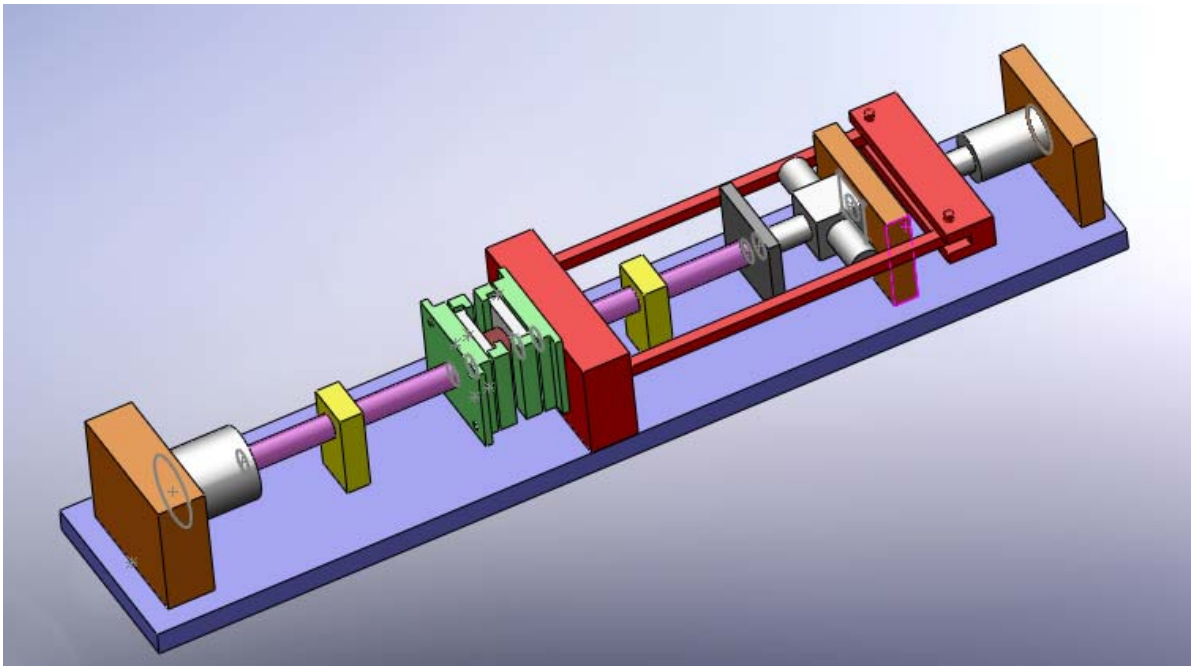

Figure 6: A picture created in Solidworks 2008 shows a design option with the compressive setup. The blue shows the base; purple shows the rods; the orange shows the supports; the green shows the grips; the gray shows the PMMA; the red shows the motion segment; the black shows the rotating rectangle; the silver shows the devices (load cell, rotary actuator, hydrualic cylinder); the yellow shows the bearing supports; the bright red shows the compression setup.

The current design, shown in Figure 7, is a combination of the previous two options shown in Figure 5 and Figure 6. The compressive hydraulic cylinder will apply compression to the rotary actuator support. The rotary actuator support will be part of the compressive setup, having the 0.5-inch square rods extending from the rotary actuator support to the PVC rectangular block located adjacent to the grips. This design allows the Delrin rod and the PVC block applying compression, and eliminates the need for the Delrin rod to extend. It is possible that the rotary actuator may be too heavy and try to tip over. If this is the case, a shelf for the rotary actuator support can be attached to the vertical support shown in Figures 5-7. Note that the PBS bath is not shown in any of the figures.

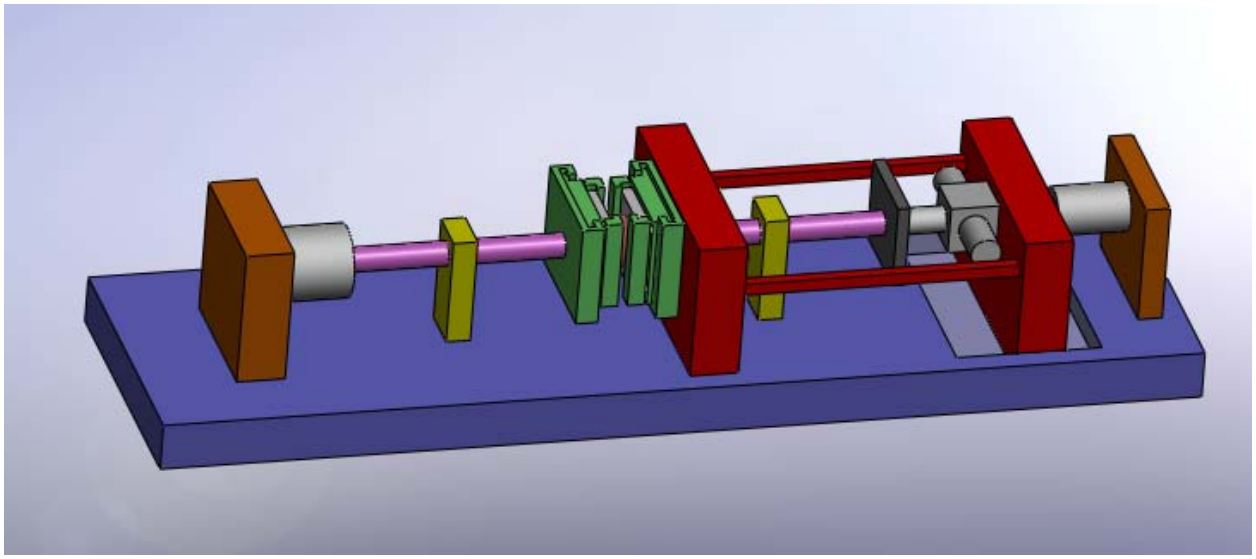

Figure 7: A picture created in Solidworks 2008 shows the current design option with the compressive setup. The blue shows the base; purple shows the rods; the orange shows the supports; the green shows the grips; the gray shows the PMMA; the red shows the motion segment; the black shows the rotating rectangle; the silver shows the devices (load cell, rotary actuator, hydrualic cylinder); the yellow shows the bearing supports; the bright red shows the compression setup.

3.3 Magnetic Resonance Imaging

For this study, either a 3T or a 7T MRI scanner (Siemens Medical Solutions) will be used. The 7T would give a better quality images than the 3T, but due to the 7T MRI scanner's intensity, it would make the device larger than desired because the metal devices would have to be placed further away from the specimen. O'Connell *et al.* used a 3T MRI scanner (Trio, Siemens Medical Solutions), and the quality of the images was sufficient for that study's strain analysis [11]. Therefore, the 3T should produce images with a high enough resolution for strain analysis. However, the decision has not been made at this point. The sequence that will be used during the test will be a high resolution The sequence that will be used will most likely be a high resolution T_2-weighted turbo spin echo.

Working in collaboration with this project are Alex Wright, PhD and James Gee, PhD from the Radiology department at the University of Pennsylvania. They are both working on ANTS. For pure compression, two-dimensional (2D) images can be taken, and those images will be sufficient for the strain analysis. However, for torsion 3D images will be needed because some of the points that are in a 2D plane initially will rotate out of the 2D plane when in torsion. In order to measure the strain, it is necessary to have an initial point and be able to trace its motion; therefore, 3D imaging is necessary.

3.3.1 Minimal Distance Protocol

Before the actual testing begins and the designs are finalized, the required minimum distances between the devices and the specimen need to be determined. In order to do this, the exact devices that will be used in the actual testing, as well as the same MRI machine, need to be used in the following protocol. The minimum distances for the devices will be different in the 3T machine than the 7T machine; therefore, it is necessary to use the appropriate machine. Also, the sequence that will be used for the actual testing should be used in this protocol.

A homogenous solution, such as water or PBS, will be placed in the MRI machine in place of a specimen. One of the devices will be placed on the appropriate side of the homogenous solution, in the same orientation that it will be in the device, and then an image will be taken. The image quality will be observed. If there is interference, the device will be moved further away from the solution; if there is no interference, the device should be moved closer to the solution. Another image will be taken, and the image quality will be observed. This process should be repeated until the minimum distance is known for each device. Once the minimum distance has been determined for each device separately, all the devices should be put in the machine with the homogenous solution at the same time on their appropriate sides. Note that either the rotary actuator or the compressive hydraulic cylinder will most likely have to be placed further than their minimum distance in order to have the same order as they would in the actual testing. The rotary actuator should be closer to the solution than the compressive hydraulic cylinder. The distance between the rotary actuator and the hydraulic cylinder depends on the design chosen. If the design has not been chosen, use a gap of approximately 1 inch between the rotary actuator and the rod of the hydraulic cylinder. An inch gap would be the closest the two objects would be together for either design option. An image should be taken with all devices in place to make sure there is no interference. If there is interference, move the appropriate device(s) until there is no interference.

3.4 Protocol

Before testing the specimens begins, the load cell will be calibrated in torsion and compression by applying known forces using an Instron testing machine (Model 8874). The rotary actuator and the hydraulic cylinder will be calibrated by placing a load cell in place of the specimen (Dyancell, Instron). A preload of 750 N will be applied and held for one hour. For a human disc, 750 N corresponds to an average of 0.48 MPa stress; this stress is equivalent to the stress felt during low to moderate activity, such as walking or

sitting. After the one-hour hold, 20 sinusoidal cycles from ±6° at 0.5 Hz will be applied while keeping the compressive load constant. The preload and preconditioning will be done using an Instron (Canton, MA) testing machine (Model 8874).

One of the preliminary tests consisted of testing a bovine tail motion segment. The specimen was preloaded to 365 N to achieve a stress of approximately 0.48 MPa. The specimen was preconditioned as previously described. The specimen was then rotated, incrementally, to 2°, 4°, and 6°. The specimen was allowed to relax at the incremental rotations. This preliminary test was done to determine the time needed for stress-relaxation of the specimen to occur. The specimen needs to have time to "relax" in order to reduce the amount of movement during imaging. Figure 8 below shows a picture of the testing setup, and Figure 9 below shows the stress-relaxation curves for all the displacement holds from this test.

Figure 8: A picture of the test setup for the preliminary test. This picture does not show the complete PBS bath.

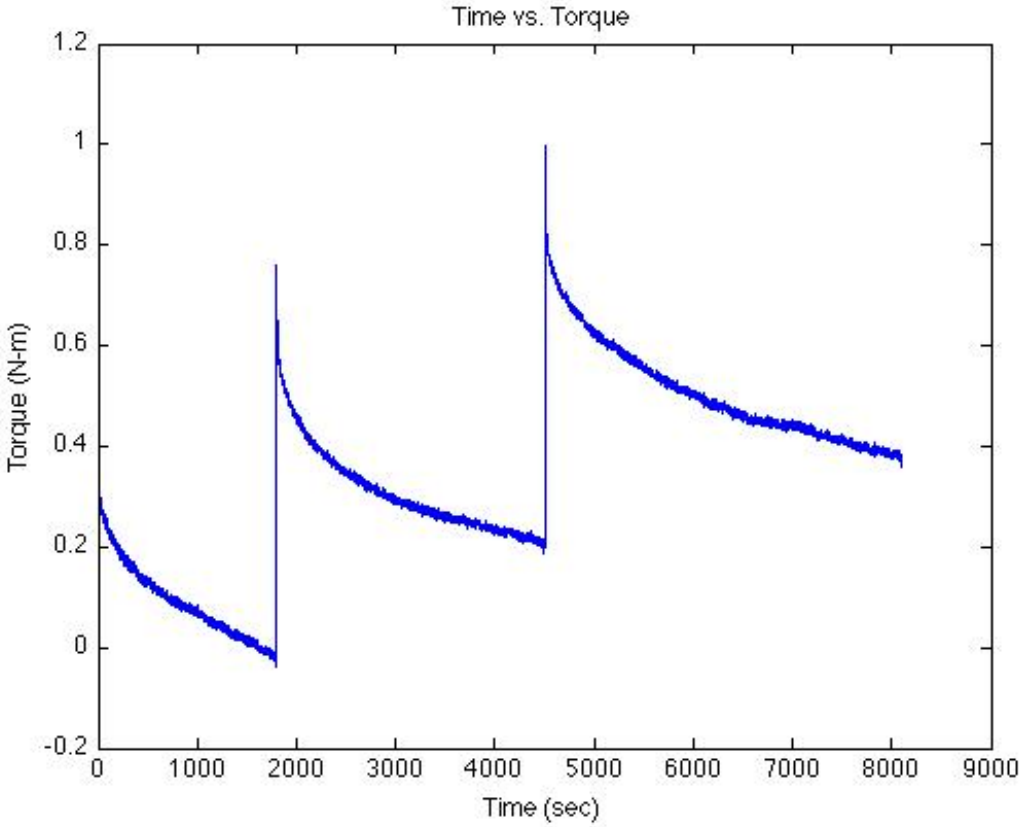

Figure 9: Stress-relaxation curves for the 2°, 4°, and 6° rotation holds from the preliminary test. Note that the specimen does not fully relax for any of the holds.

After analyzing the data from the preliminary test and developing Figure 9, it was determined that the specimen did not fully relax for any of the holds. Therefore, the times for the actual test have not been determined. Another preliminary test will be ran that will hold the angle displacements longer in order to determine the equilibrium time.

For the actual test, a constant force of approximately 750 N will be applied by the hydraulic cylinder throughout the duration of the test. The specimen will then be rotated to a displacement of 2°, then 4°, and then 6°. The holding times for each angle displacement will be chosen based on the preliminary test results.

3.5 Data Analysis

While MRI is a useful tool for imaging specimens, it does not output displacement or strain. In a previous study, O'Connell *et al* [11], texture correlation was used to find the displacements between a reference image and a deformed image. The strain can be calculated from the displacement. This method is an accepted method, and has low strain percent error when used with MR images [26]. However, for this study ANTS will be used instead of texture correlation.

4. RECOMMENDATIONS

The goal of this research project is to study the mechanical properties of the disc; therefore, the disc was isolated. Future work could include studying discs that are not isolated. Leaving all the joints and ligaments intact and applying compression and torsion would lead to a better understanding of the properties of the entire spine. If the joints and ligaments are left intact, the amount of torque applied should be increased since the intact structure can resist a larger load than an isolated disc [12]. Knowing the properties of both the isolated and non-isolated disc could be very advantageous in future motion segment studies.

5. CONCLUSIONS

In conclusion, a non-magnetic device has been designed to apply torsion and compression to a specimen, with the exception of some dimensions. The design will not be finalized until the minimum distance for the metal devices have been determined by following the protocol in Section 3.3.1. The device will not be built until the design is finalized and a Delrin rod has been tested to ensure that it can resist the torque that will be applied. A hydraulic cylinder (URR-17-1/2, Clippard Minimatic) will be used to apply the compression, and a custom-built load cell (LXT-920, Cooper Instruments) will be used in the device that will measure the torsion and compression throughout the test. A custom-built rotary actuator (Bimba) is being designed but some details on controlling the amount of rotation are still being worked on before finalizing the design. When these three devices are available, the preliminary distance test can be conducted. Once the device is built, the plan is to proceed to test the specimens with the protocol described in Section 3.4.

6. ACKNOWLEDGEMENTS

I would like to thank many organizations and people for their help and support throughout this summer. I would like to thank the SUNFEST program director, Jan Van der Spiegel, the Electrical and Systems Engineering Department at the University of Pennsylvania for hosting the SUNFEST program, and I would also like to thank the National Science Foundation for the grant that funds the SUNFEST program.

I also want to thank the McKay Orthopedic Research Lab, which is the lab that I worked in this summer. Specifically, I would like to thank my advisor Dr. Dawn Elliot, and Jonathon Yoder, a graduate student whom I worked closely with throughout the summer.

7. REFERENCES

[1] M. A. Adams, and P. Dolan. (2005, Oct.). Spine biomechanics. *Journal of Biomechanics*. [Online]. *38 (10),* pp. 1972-1983. Available: http://www.ncbi.nlm.nih.gov/pubmed/15936025

[2] M. A. Adams, and P. J. Roughley. (2006, Sept.). What is Intervertebral Disc Degeneration, and What Causes It?. *Spine*. [Online]. *31 (18)* pp. 2151-2161. Available: http://www.medscape.com/viewarticle/543611

[3] Degenerative Disc Disease. (2009). Medtronic. [Online]. Available: http://wwwp.medtronic.com/Newsroom/LinkedItemDetails.do?itemId=1101769745199&itemType=fact_sheet&lang=en_US

[4] American Chriopractic Association. (2009). [Online]. Available: http://www.acatoday.org/level2_css.cfm?T1ID=13&T2ID=68

[5] M. B. Coventry, R. K. Ghormley, and J. W. Kernohan. (1945, Jan.). The Intervertebral Disc: Its Microscopic Anatomy and Pathology. *The Journal of Bone and Joint Surgery*. [Online]. *27 (1)* pp. 105-112. Available: http://www.ejbjs.org/cgi/reprint/27/1/105

[6] H. F. Farfan, J. W. Cossette, G. H. Robertson, R. V. Wells, and H. Kraus. (1970, April). The Effects of Torsion on the Lumbar Intervertebral Joints: The Role of Torsion in the Production of Disc Degeneration. *The Journal of Bone and Joint Surgery*. [Online]. *52 (3),* pp. 468-497. Available: http://www.ejbjs.org/cgi/content/abstract/52/3/468

[7] V. M. Haughton, T. H. Lim, and H. An. (1999, June). Intervertebral Disk Appearance Correlated with Stiffness of Lumbar Spinal Motion Segments. *American Journal of Neuroradiol*ogy. [Online]. *20 (6),* pp. 1161-1165. Available: http://www.ajnr.org/cgi/reprint/20/6/1161.pdf

[8] T. A. Schmidt, H. S. An, T. H. Lim, B. H. Nowicki, V. M. Haughton. (1998, Oct.). The Stiffness of Lumbar Spinal Motion Segments With a High-Intensity Zone in the Annulus Fibrosis. *Spine*. [Online]. *23 (20),* pp. 2167-2173. Available: http://ovid.tx.ovid.com/spa/ovidweb.cgi

[9] A. Fujiwara, T. H. Lim, H. S. An, N. Tanaka, C. H. Jeon, G. B. J. Andersson, V. M. Haughton. (2000, Dec.). The Effect of Disc Degeneration and Facet Joint Osteoarthritis on the Segmental Flexibility of the Lumbar Spine. *Spine*. [Online]. *25 (23),* pp. 3036-3044. Available: http://www.ncbi.nlm.nih.gov/pubmed/11145815

[10] K. M. McGlashen, J. A. A. Miller, A. B. Schultz, and G. B. J. Andersson. (1987). Load Displacement Behavior of the Human Lumbo-sacral Joint. *Journal of Orthopedic Research*. [Online]. *5 (4),* pp. 488-496. Avaiable: http://deepblue.lib.umich.edu/handle/2027.42/50380

[11] G. D. O'Connell, W. Johannessen, E. J. Vresilovic, and D. M. Elliot. (2007, Dec.). Human Internal Disc Strains in Axial Compression Measured Noninvasively Using Magnetic Resonance Imaging. *Spine*. [Online]. *32 (25),* pp. 2860-2868. Available: http://cat.inist.fr/?aModele=afficheN&cpsidt=19897075

[12] M. A. Adams, and W. C. Hutton. (1981, Jun). The relevance of torsion to the mechanical derangement of the lumbar spine. *Spine*. [Online]. *6 (3)*, pp. 241-248. Available: http://www.ncbi.nlm.nih.gov/pubmed/7268544

[13] D. M. Gillard. (2005). Degenerative Disc Disease (DDD). [Online]. Available: http://www.chirogeek.com/000_DDD_Page-1_Aging.htm

[14] A. N. Nguyen, W. Johannessen, J. H. Yoder, A. J. Wheaton, E. J. Vresilovic, A. Borthakur, D. M. Elliot. (2008, April). Noninvasive Quantification of Human Nucleus Pulposus Pressure with Use of T1ρ-Weighted Magnetic Resonance Imaging. *The Journal of Bone and Joint Surgery*. [Online]. *90 (4)*, pp. 796-802. Avaliable: http://www.pubmedcentral.nih.gov/articlerender.fcgi?artid=2657301

[15] J. D. Auerbach, W. Johannessen, A. Borthakur, A. J. Wheaton, C. A. Dolinskas, R. A. Balderston, R. Reddy, and D. M. Elliot. (2006, Aug.). In vivo quantification of human lumbar disc degeneration using $T_{1\rho}$-weighted magnetic resonance imaging. *Spine*. [Online]. *15 (3)*, pp. 338-344. Available: http://www.pubmedcentral.nih.gov/articlerender.fcgi?artid=2335378

[16] W. Johannessen, J. D. Auderbach, A. J. Wheaton, A. Kurji, A. Borthakur, R. Reddy, D. M. Elliot. (2006, May). Assessment of Human Disc Degeneration and Proteoglycan Content Using $T_{1\rho}$-weighted Magnetic Resonance Imaging. *Spine* [Online]. *31 (11)*, pp. 1253-1257. Available: http://cat.inist.fr/?aModele=afficheN&cpsidt=17811514

[17] M. A. Adams, P. Dolan, W. C. Hutton, and R. W. Porter. (1990, Mar.). Diurnal Changes in Spinal Mechanics and Their Clinical Significance. *The Journal of Bone and Joint Surgery*. [Online]. *72 (2)*, pp. 266-270. Available: http://www.jbjs.org.uk/cgi/content/abstract/72-B/2/266

[18] EURODISC. Intervertebral Disc Degeneration: Interplay of Age, Environmental and Genetic Factors.[Online]. Available: http://www.physiol.ox.ac.uk/EURODISC

[19] B. Ludescher, J. Effelsberg, P. Martiosian, G. Steidle, B. Markert, C. Claussen, and F. Schick. (2008, July). T2- and Diffusion-Maps Reveal Diurnal Changs of Intevertebral Disc Composition: An In Vivo MRI Study at 1.5 Tesla. *Journal of Magnetic Resonance Imaging*. [Online]. *28 (1)*, pp. 252-257. Available: http://www.ncbi.nlm.nih.gov/pubmed/18581387

[20] N. Boos, Å. Wallin, T. Gbedegbegnon, M. Aebi, and C. Boesch. (1993, Aug.) Quantitative MR Imaging of Lumbar Intervertebral Disks and Vertebral Bodies: Influence of Diurnal Water Content Variations. *Radiology*. [Online]. *188 (2)*, pp. 351-354. Available: http://radiology.rsnajnls.org/cgi/content/abstract/188/2/351

[21] J. R. Ledsome, V. Lessoway, L. E. Susak, F. A. Gagnon, R. D. Gagnon, and P. C. Wing. (1996, July). Diurnal Changes in Lumbar Intervertebral Distance, Measured Using Ultrasound. *Spine*. [Online]. *21 (14)*, pp. 1671-1675. Available: http://cat.inist.fr/?aModele=afficheN&cpsidt=3174283

[22] J. A. Malko, W. C. Hutton, and W. A. Fajman. (1999, May). An *In Vivo* Magnetic Resonance Imaging Study of Changes in the Volume (and Fluid Content) of the Lumbar Intervertebral Discs During a Simulated Diurnal

Load Cycle. *Spine*. [Online]. *24 (10)*, pp. 1015-1022. Available: http://cat.inist.fr/?aModele=afficheN&cpsidt=1792648

[23] N. Boos, A. Wallin, M. Aebi, and C. Boesch. (1996, March). A New Magnetic Resonance Imaging Analysis Method for the Measurement of Disc Height Variations. *Spine*. [Online]. *21 (5)*, pp. 563-570. Available: http://www.ncbi.nlm.nih.gov/pubmed/8852310

[24] E. J. Chiu, D. C. Newitt, M. R. Segal, S. S. Hu, J. C. Lotz, and S. Majumdar. (2001, March). Magnetic Resonance Imaging Measurement of Relaxation and Water Diffusion in the Human Lumbar Intervertebral Disc Under Compression In Vitro. *Spine*. [Online]. *26 (19)*, pp. E437-E444. Avaliable: http://www.ncbi.nlm.nih.gov/pubmed/11698903

[25] M. J. Bey, H. E. Song, F. W. Wehrli, and L. J. Soslowsky. (2002, July). Intratendinous strain fields of the intact supraspinatus tendon: the effect of glenohumeral joint position and tendon region. *Journal of Orthopedic Surgery*. [Online]. *20 (4)*, pp. 869-874. Avaliable: http://cat.inist.fr/?aModele=afficheN&cpsidt=13834515

[26] M. J. Bey, H. K. Song, F. W. Wehrli, and L. J. Soslowsky. (2002, April). A Noncontact, Nondestructive Method for Quantifying Intratissue Deformations and Strains. *Journal of Biomechanical Engineering*. [Online]. *124 (2)*, pp. 253-258. Available: http://www.ncbi.nlm.nih.gov/pubmed/12002136

[27] C. L. Gilchrist, W. W. Witvoet-Braam, F. Guilak, and L.A. Setton. (2006, March). Measurement of intracellular strain on deformable substrates with texture correlation. *Journal of Biomechanics*. [Online]. *40 (4)*, pp. 786-794. Available: http://www.jbiomech.com/article/S0021-9290(06)00107-2/abstract

[28] C. L. Gilchrist, J. Q. Xia, L. A. Setton, and E. W. Hsu. (2004, May). High-resolution determination of soft tissue deformations using MRI and first-order texture correlation. *IEEE Transactions on Medical Imaging*. [Online]. *23 (5)*, pp. 546-553. Available: http://ieeexplore.ieee.org/stamp/stamp.jsp?arnumber=01295075

[29] C. W. Pfirrmann, A. Metzdorf, M. Zanetti, J. Hodler, and N. Boos. (2001, Sept.). Magnetic resonance classification of lumbar intervertebral disc degeneration. *Spine*. [Online]. *26 (17)*, pp. 1873-1878. Available: http://www.ncbi.nlm.nih.gov/pubmed/11568697